Single Carrier Optical FDM in Visible Light Communication

Osama Saied[1], Zabih Ghassemlooy[1], Refik Caglar Kizilirmak[2], Xuewu Dai[1], Carlos Ribeiro[3], Min. Zhang [4] ,and Sujan Rajbhandari[5]
[1]Optical Communications Research Group, NCRLab, Faculty of Engineering and Environment, Northumbria University, Newcastle Upon Tyne, NE1 8ST, UK
{osama.saied, z.ghassemlooy, xuewu.dai}@northumbria.ac.uk
[2]Dept. of Electrical and Electronics Engineering Nazarbayev University Astana, Kazakhstan,
refik.kizilirmak@nu.edu.kz
[3]Instituto de Telecomunicacoes, Instituto Politecnico de Leiria, Leiria, Portugal
carlos.ribeiro@ipleiria.pt
[4]The State Key Laboratory of Information Photonics and Optical Communications, Beijing University of Posts & Telecommunications, Beijing,
mzhang@bupt.edu.cn
[5]School of Computing, Electronics and Mathematics, Coventry University
ac1378@coventry.ac.uk

***Abstract*—Light emitting diodes (LEDs) used in visible light communications (VLC) have a limited optical power-current linear range, which could be a problem in multi-level and multi-carrier frequency modulation schemes. Orthogonal frequency division multiplexing (OFDM) as a popular scheme in VLC suffers from nonlinear distortion due to the high peak to average power ratio (PAPR). In this paper, we present a novel single carrier optical frequency division multiplexing signaling scheme for VLC, where the symmetrical characteristics of single carrier frequency division multiple access is investigated in order to reduce PAPR. Simulation results show that PAPR reduced by 10 dB compared to the traditional asymmetrically clipped optical OFDM. We show that the bit-error-rate performance of the proposed scheme is enhanced compared to ACO-OFDM when the limited dynamic range of digital to analog converter and LED is considered.**

Keywords— OFDM; PAPR; visible light communications.

I. INTRODUCTION

Visible light communications (VLC) is an attractive technique that uses white light emitting diodes (WLEDs) to provide illumination, data communications, indoor localization as well as remote sensing in the visible wavelength range [1]. Thought visible wavelength from 380 to 780 nm offers a bandwidth of 300 THz, the modulation bandwidth of the WLEDs is limited a few MHz due to long photoluminescence lifetime (~ μs) of yellow phosphors. Therefore, a blue filtering (to filter out the slow yellow components at the receiver (Rx)), complex modulation scheme as well as equalization have been used to increase the transmission capacity of the WLED [2], [3].

Although the delay spread of the indoor VLC channel is rather small for a typical room, there are high error probability at the edges and corners of a room due to multipath reflections[4]. To compensate the inter symbol interference (ISI) due to the slow LED response, multipath propagations, a number of modulation schemes had been considered for VLC system. Among them, pulse amplitude modulation (PAM) with equalization, carrier-less amplitude and phase (CAP) and orthogonal frequency division multiplexing (OFDM) are adopted for practical demonstration. OFDM scheme have been extensively investigated for high-speed communications due to its ability to support higher data rates and multi-user, and its efficiency to combat ISI [3], [4], [5]. The conventional OFDM signal, which is both bipolar and complex signals, must be modified to intensity modulation (IM) of LEDs. Thus, DC-biased optical OFDM (DCO-OFDM) and asymmetrically clipped optical OFDM (ACO-OFDM) have emerged as the most popular OFDM schemes adopted in IM/ direct detection (DD) VLC systems [6], [7]. In order to generate real-time domain signals a real signal, a Hermitian symmetry (HS) is imposed. This will reduce the spectral efficiency to half in comparison to conventional OFDM of half of the available bandwidth [6], [8]. Since only the odd sub-carriers are modulated in ACO-OFDM, clipping the negative time domain samples do not cause any loss of information [6].

However, the real time domain signal can also be accrued by transmitting the OFDM signal using two symbols (i.e., the real and imaginary OFDM samples are transmitted by the first and second symbols, respectively) thus requiring reduced IFFT points compared to HS [9].

Though OFDM offers a number of advantages, its performance is adversely affect by non-linear distortion (from LEDs) and the limited digital-to-analog converter dynamic range (DACDR) due to the high peak to average power ratio (PAPR) [10], [11]. In VLC systems, signal extending beyond the LED's linear range will experience not-linear distortion, thus resulting in a high bit error probability [1], [5]. A number of techniques have been reported to address the high PAPR in optical OFDM [12]-[15]. Recently, single carrier frequency division multiple accesses (SC-FDMA) was adopted for the IM/DD based VLC system to improve PAPR [16]-[18]. A LED array with SC-FDMA was implemented in [16] to reduce OFDM PAPR on VLC at a cost of the transmission rate per LED transmitter due to the interleaving and localized mapping implementation. ACO-single carrier frequency domain equalization (ACO-SCFDE) and repetition and clipping optical SCFDE (RCO-SCFDE), were presented in [17] and [18],

respectively as two modified SC-FDMA schemes with the same data rates per single LED transmitter (Tx) as in ACO-OFDM. The only difference between ACO-SCFDE and the traditional ACO-OFDM is the additional FFT and IFFT blocks at the Tx and the Rx, respectively. Unlike ACO-SCFDE with modulation of only the odd SCs, in RCO-SCFDE the real OFDM signal is transmitted via two blocks. The first block is used to transmit the real positive samples, whereas the negative real samples are transmitted by the second block. Thus achieving reduced IFFT length compared to ACO-SCFDE [17], [18]. However, in order to present a real OFDM signal all the above modified SC-FDMA schemes must adhere to HS, which leads to higher PAPR compared to SC-FDMA in the radio frequency (RF) domain since only half of the OFDM subcarriers enjoy the mapping feature [16].

In this paper, SC-FDMA is adopted for the IM/DD based VLC system with no HS requirement, which offer significantly improved PAPR. Due to the interleaving mapping of the SC-FDMA frequency domain signal, the output time domain samples of the IFFT will be asymmetrically repeated Q-time over the SC-FDMA symbol period, where Q is the interleaving mapping factor [19]. The symmetrical characteristic of SC-FDMA is investigated by setting Q = 4. Here, each time-domain OFDM symbol is divided into four sub-symbols where the 1st, 2nd, 3rd and 4th sub-symbols carry positive values of the real samples r_+, positive values of imaginary samples i_+, negative values of real samples r_- and the negative values of imaginary samples i_-, respectively. In this work, this process is referred to as intensity modulation process (IMP). Simulation results show that PAPR of the proposed scheme is 10 dB and 8dB lower than the traditional ACO-OFDM and ACO-SCFDE respectively. We also show that the BER performance of the proposed scheme is further improved compared with ACO-OFDM and ACO-SCFDE when limited dynamic range of the LED and DAC are considered.

The rest of the paper is organized as follows; Section II presents the proposed single carrier optical frequency division multiplexing (SCO-FDM) scheme. Results obtained for the proposed scheme are analyzed and evaluated in Section III. Finally, conclusions are drawn in Section IV.

II. Single Carrier Optical FDM (SCO-FDM)

The analysis of the proposed SCO-FDM system, including the structures of both the Tx and Rx is presented in this section. The interleaving mapping is investigated in this study to make SC-FDMA applicable for IM/DD VLC systems.

A. Transmitter

Fig. 1 depicts the block diagram of the Tx for SCO-FDM, which is similar to the standard SC-FDMA. The main difference being the inclusion of IMP book at Tx. Whereas, intensity demodulation process (IDP) block is inserted at the Rx. The signal processing steps at the Tx are described as follows. First, the serial binary bits $b_i(t)$ are converted into parallel data streams and mapped onto a group of complex quadrature amplitude modulation (QAM) symbols x_k as given by:

$$x_k = [x_0, x_1, x_2, \dots x_{M-1}], \tag{1}$$

where M is the number of data symbols. The complex symbols are transformed to the frequency domain by the FFT block and its output in the frequency domain is given as:

$$X_m = \sum_{k=0}^{M-1} x_k \ \mathrm{e}^{-j2\Pi\frac{k}{M}m}, \tag{2}$$

where X_m, refers to the symbol at the m^{th} sub-carrier, $m =$

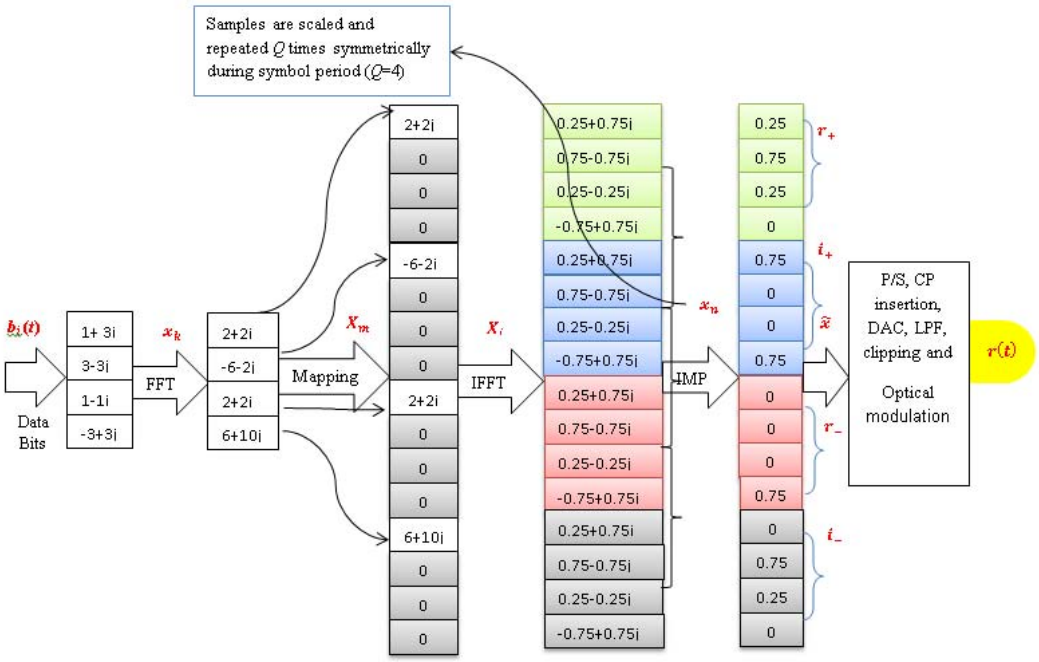

Fig.1 Block of SCO-FDM Transmitter

$\{0,1,2,\ldots..M-1\}$, and $X=[X_1\ X_2\cdots X_M]^T\in\mathbb{C}^M$ (note that $\mathbb{C}^M$denotes the set of M-dimensional complex numbers). Interleaving mapping is carried out on X_m by inserting $(Q-1)$ number of zeros between the adjacent sub-carriers (here, $Q=4$, see Fig. 1). The mapped output signal is defined as:

$$X_i=\begin{cases}X_m, & \text{if } i=Qm \text{ where } 0\le m\le M-1\\ 0, & \text{otherwise}\end{cases}, \tag{3}$$

$i=\{0,1,2,\ldots.N-1\}$, and $N=QM$. The mapped frequency domain signal is then converted back to the time domain signal given as:

$$x_n=\frac{1}{N}\sum_{i=0}^{N-1}X_i\,e^{j2\Pi\frac{i}{N}n}, \tag{4}$$

where,x_n $(x\in\mathbb{C}^N)$ refers to the n^{th} time domain sample and $n=\{0,1,2,\ldots.N-1\}$. By letting $n=(Mq+m)$ for $0\le q\le Q-1$ in (4), we obtain [15]:

$$\begin{aligned}x_n=x_{Mq+m}&=\frac{1}{N}\sum_{i=0}^{N-1}X_i\,e^{j2\Pi\frac{i}{N}(Mq+m)}\\&=\frac{1}{Q}\frac{1}{M}\sum_{i=0}^{M-1}X_m\,e^{j2\Pi\frac{k}{M}m}\\&=\frac{1}{Q}\left[\frac{1}{M}\sum_{i=0}^{M-1}X_m\,e^{j2\Pi\frac{k}{M}m}\right]\\&=\frac{1}{Q}x_k.\end{aligned} \tag{5}$$

From (5), it can be clearly seen that x_n is a scaled (amplitude) version of x_k. Indeed x_n have the characteristics of a single carrier with low PAPR [15]. However, because of the interleaving mapping of X_m, by Q, x_n is repeated Q-times over a given symbol period (see Fig. 1) as:

$$x_n=x_{n+Q}=x_{n+2Q},=..,=x_{n+(Q-1).Q}. \tag{6}$$

To make SC-FDMA applicable for IM/DD VLC systems the IMP block is inserted after IFFT process, see Fig. 1, which consists of the following procedures (i) inverting the 2nd half of the OFDM symbol; (ii) removing the imaginary part of the 1st and 3rd quarters of the OFDM symbol; (iii) removing the real part of the 2nd and 4th quarters of the OFDM symbol; and (iv) remove all the negative samples. Because of the symmetrical characteristic (i.e., repetition pattern) of x_n, this whole process does not result in any loss of information. The IMP block extracts the real $[r_+,r_-]$ and the imaginary$[i_+,i_-]$ parts from x_n, and its output signal is a real unipolar signal composed of four sub-symbols given as:

where;

$$r_+=\begin{cases}\text{real } x_n, & \text{if real } x_n\ge 0\\ 0 & \text{otherwise}\end{cases}\quad \text{for } (n\le M-1).$$

$$i_+=\begin{cases}\text{imag } x_n, & \text{if imag } x_n\ge 0\\ 0 & \text{otherwise}\end{cases}\quad \text{for } (M\le n<2M).$$

$$r_-=\begin{cases}\text{real } x_n, & \text{if real } x_n<0\\ 0 & \text{otherwise}\end{cases}\quad \text{for } (2M\le n<3M).$$

$$i_-=\begin{cases}\text{imag } x_n, & \text{if imag } x_n<0\\ 0 & \text{otherwise}\end{cases}\quad \text{for}(3M\le n<N-1).$$

Note that the transmitted signal has the same symbol rate as the traditional ACO-OFDM. Finally, $\tilde{x}$ is passed through parallel to serial (P/S), cyclic prefix (CP) insertion, digital to analog converter (DAC), low pass filter (LPF), and clipping modules prior to IM of LEDs. Note that SCO-FDM is in the real unipolar format.

B. Receiver

Fig. 2 illustrates the block diagram of the SCO-FDM Rx with functionality opposite to the Tx. Without loss of generality, we set the channel gain from optical source to photodiode at one. Then the received signal in electrical domain, assuming no clipping distortion in the system, can be written as: $y(t)=r(t)+w_n(t)$, where $r(t)$ is the electrical information waveform after optical electrical conversion (O/E), $w_n(t)$ is additive Gaussian noise with mean zero and variance σ_n^2. $y(t)$ is then converted into the digital signal x_d by being passed through a LPF, analog to digital converter (ADC), CP removal and S/P modules. Then, x_d is processed in the intensity demodulation process (IDP) block where the original complex and repeated samples (i.e., x_n added by noise) will be reconstructed. The output of IDP is passed through FFT, interleaving de-mapping, IFFT, QAM de-mapping and P/S blocks to reconstruct the information bits.

III. Simulation Results

We have considered 1024-point IFFT and 16-QAM. The LED bandwidth is 20 MHz and the cyclic prefix duration is 50

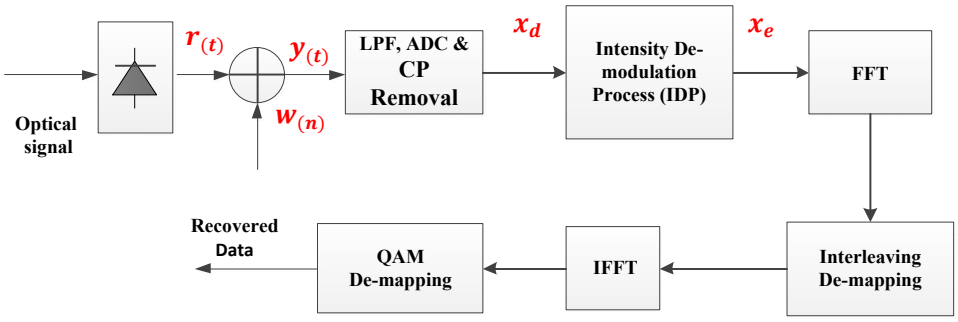

Figure 2 Block diagram of SCO-FDM

ns, which is the maximum time delay for indoor VLC multipath channel [20]. The PAPR for all OFDM schemes is calculated as [19] $\text{PAPR} = \frac{\text{peak power of } x(t)}{\text{average power of } x(t)}$, where $x(t)$ is the time domain signal after IFFT block for ACO-OFDM and ACO-SCFDE schemes. For the proposed scheme, on the other hand, $x(t)$ is the time domain signal after the IMP block. Complementary cumulative distribution function (CCDF) of PAPR, represented by $\Pr\{\text{PAPR} > \text{PAPR}_0\}$, is the probability that PAPR is higher than a certain PARP threshold PAPR_0, thus CCDF is determined by means of Monte Carlo simulation [15]. CCDF results of PAPR for ACO-OFDM, ACO-SCFDE and SCO-FDM are evaluated and compared in Fig. 3. We compare the PAPR value that exceeded with the probability < 0.01% ($\Pr\{\text{PAPR} > \text{PAPR}_0\} = 10^{-4}$).

From Fig. 3, it can be seen that for SCO-FDM and ACO-SCFDE, PAPRs are lower than the traditional ACO-OFDM by 10 dB and 3 dB, respectively. In ACO-SCFDE the improvement is due to implementation of FFT and interleaving mapping blocks before the HS process at the Tx. In the proposed SCO-FDM scheme, by implementing the FFT and the interleaving mapping blocks before the IFFT block results in significantly reduced PAPR.

Fig. 4 shows the BER performance as a function of DAC dynamic range for ACO-OFDM, ACO-SCFDE and SCO-FDM for the signal to noise ratio (SNR) of 10 dB. It can be seen that when the DACDR is wide (i.e., > 40 dB), all the three schemes display the same BER performance. This is expected since there is no distortion due to the wide DACDR. The BER of 1.6×10^{-2} is the minimum achievable for the SNR of 10 dB. When DACDR is <40 dB all three schemes show different BER profile, with the proposed SCO-FDM scheme displaying lower BER performance.

Fig. 5 depicts the BER performance as a function of the average signal power for the above mentioned schemes for an LED with a limited dynamic range. In order to observe only the effect of the limited dynamic range of the LED on the BER performance, we assumed an unlimited DACDR. In the analysis, the turn on voltage (V_{tov}) and the maximum allowed forward voltage (V_{max}) of the LED are taken as 3 and 3.75 V, respectively, and σ_n^2 is set at -10 dBm. For all three schemes when the average power of the electrical signals < 15 dBm, we observe no clipping distortion and the same BER performance. For the signal power > 15 dBm, the amplitude levels of ACO-OFDM and ACO-SCFDE exceed the dynamic range of the LED, thus noticing degradation in the BER performances due to the clipping distortion. For SCO-FDM, on the other hand, there is no clipping distortion up to 20 dBm, beyond which clipping and thus BER performance degradation is observed.

IV. Conclusion

In this paper, the symmetrical time domain characteristics of SC-FDMA were adopted for the IM/DD VLC system. A novel technique known as SCO-FDM was proposed to reduce PAPR in the conventional OFDM. This was achieved by letting SC-FDMA time domain samples, repeated 4 times symmetrically during each SC-FDMA time domain symbol period by setting the interleaving mapping factor at frequency domain to 4. The simulation results showed that the PAPR value of the proposed scheme is 10 dB lower than that of the ACO-OFDM. The impact of reduced PAPR on the system performance was investigated by incorporating the dynamic range of the both digital-to-analog-converter (DACDR) and LED. It was shown that, the DACDR performance was enhanced by almost 6 dB when the new scheme was implemented. When considering the dynamic range of LED, the achievable minimum BER for SCO-FDM was found to be lower than those of ACO-OFDM and ACO-SCFDE.

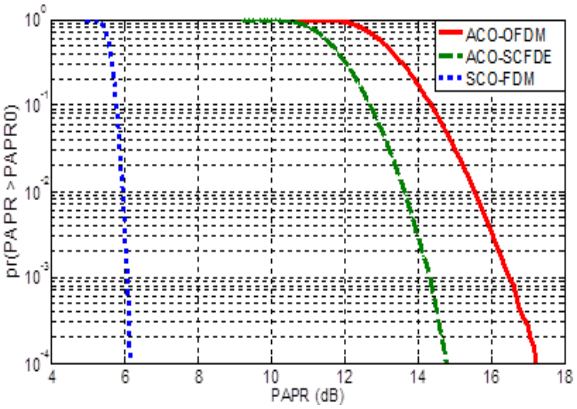

Fig. 3 CCDF vs PAPR for ACO-OFDM, ACO-SCFDE and SCO-FDM

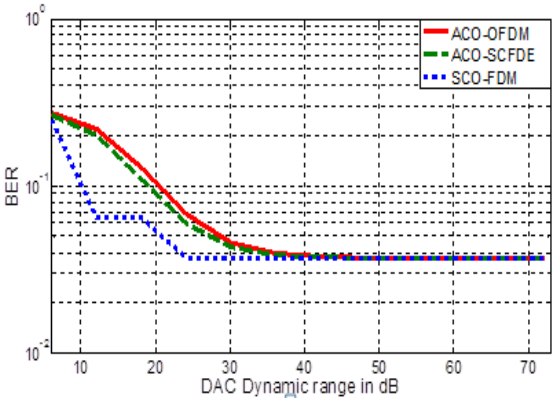

Fig. 4 DACDR vs BER for ACO-OFDM, ACO-SCFDE and SCO-FDM

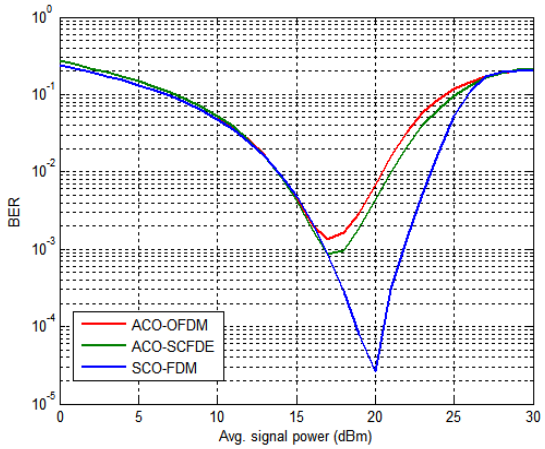

Fig. 5 BER performance against the average signal power for ACO-OFDM, ACO-SCFDE and OSC-FDM

ACKNOWLEDGMENT

This work was supported by the EU Cost Action IC1101 and Portuguese FCT/MEC through national funds and when applicable co-funded by FEDER – PT2020 partnership agreement under the project UID/EEA/50008/2013. The first author acknowledges and greatly appreciates the financial support received from the Ministry of Education in Libya and the Biruni Remote Sensing Center (BRSC). The work of Carlos Ribeiro was financially supported by Portuguese FCT/MEC and its funding program under the postdoctoral grant SFRH/BPD/104212/2014.

REFERENCES

[1] Z. Ghassemlooy, W. Popoola, and S. Rajbhandari, *Optical wireless communications: system and channel modelling with Matlab*. London,UK:CRC Press, 2013.

[2] J. Grubor, K.-D. Langer, S. C. J. Lee, T. Koonen, and J. W. Walewski, "Wireless high-speed data transmission with phosphorescent white-light LEDs*," in Proc. 33rd Eur. Conf. Exhib. Opt. Commun*, 2007,pp. 1–2.

[3] S. Dimitrov and H. Haas, *Principles of LED Light Communications: Towards Networked Li-Fi*: Cambridge University Press, 2015.

[4] M. Aminikashani, W. Gu, and M. Kavehrad, "Indoor Location Estimation with Optical-based OFDM Communications," *arXiv:1505.01811,* 2015.

[5] Y. Bingyan, Z. Hongming, W. Ling, and S. Jian, "Subcarrier Grouping OFDM for Visible-Light Communication Systems," *IEEE Photonics Journal* , vol. 7, 2015, pp.1-12.

[6] S. D. Dissanayake and J. Armstrong, "Comparison of ACO-OFDM, DCO-OFDM and ADO-OFDM in IM/DD systems," *Journal of Lightwave Technology*, vol. 31, 2013, pp. 1063-1072.

[7] F. Barrami, Y. Le Guennec, E. Novakov, and P. Busson, "An optical power efficient asymmetrically companded DCO-OFDM for IM/DD systems," *in 23rd Wireless and Optical Communication Conference (WOCC)*, 2014, pp. 1-6.

[8] J. Armstrong and B. Schmidt, "Comparison of asymmetrically clipped optical OFDM and DC-biased optical OFDM in AWGN," *IEEE Communications Letter* , vol. 12, 2008, pp. 343-345.

[9] Fatima Barrami, et al., "A novel FFT/IFFT size efficient technique to generate real time optical OFDM signals compatible with IM/DD systems," *in Proc. European Microwave Conference (EuMC),* Nuremberg, Germany, 2013, pp. 1247-1250.

[10] B. Hanta, "SC-FDMA and LTE uplink physical layer design," Siminar LTE: Der Mobilfunk der Zukunft, University of Erlangen-Nuremberg, LMK, November 2009.

[11] C. R. Berger, Y. Benlachtar, and R. Killey, "Optimum clipping for optical OFDM with limited resolution DAC/ADC," *in Signal Processing in Photonic Communications,* 2011.

[12] R. You and J. Kahn, "Average power reduction technique for multiple subcarrier intensity-modulated optical signals," *IEEE Trans. Commun.*, vol. 49, no.1, ,2001, pp. 2164–2171.

[13] W. Kang and S. Hranilovic, "Power reduction techniques for multiple subcarrier modulated diffuse wireless optical channels*," IEEE Trans. Commun.*, vol. 56, no. 2, 2008, pp. 279–288.

[14] L. Nadal, M. Svaluto Moreolo, J. Fabrega, and G. Junyent, "Low complexity bit rate variable transponders based on optical OFDM with PAPR reduction capabilities," *In 17th NOC*, Spain, 2012, pp. 1–6.

[15] W.O. Popoola, Z. Ghassemlooy, and B.G. Stewart, "Pilot-assisted PAPR reduction technique for optical OFDM communication systems," *Journal of Lightwave Technology*, vol. 32, no.7, 2014, pp. 1374–1382.

[16] Chaopei Wu, Hua Zhang, Wei Xu, "On visible light communication using LED array with DFT-Spread OFDM," *IEEE International Conference on Communications (ICC)*, 2014, pp. 3325-3330,10-14.

[17] R. Mesleh, "OFDM and SCFDE performance comparison for indoor optical wireless communication systems," *in 19th International Conference on Telecommunications (ICT)*, 2012, pp. 1–5.

[18] K. Acolatse, Y. Bar-Ness, and S. K. Wilson, "Single carrier frequency domain equalization for optical wireless communications".

[19] H. G. Myung, L. Junsung, and D. Goodman, "Peak-to-average power ratio of single carrier FDMA signals with pulse shaping," *in IEEE, Personal, Indoor and Mobile Radio Communications*, 2006, pp. 1-5.

[20] H. Elgala, R. Mesleh, and H. Haas,"Practical considerations for indoor wireless optical system implementation using OFDM, " *Conference in Telecommunications*, Zagreb, Croatia, 2009, pp. 25–30.